D-Glucose-Recognition and Phlorizin-Binding Sites in Human Sodium/D-Glucose Cotransporter 1 (hSGLT1): A Tryptophan Scanning Study†

Navneet K. Tyagi,[‡,§] Azad Kumar,[‡,||] Pankaj Goyal,[⊥] Dharmendra Pandey,[⊥] Wolfgang Siess,[⊥] and Rolf K. H. Kinne*[,‡]

Max Planck Institute of Molecular Physiology, Otto-Hahn-Strasse 11, Dortmund, 44227, Germany, and the Institute for Prevention of Cardiovascular Disease, Ludwig Maximilian University, Pettenkoferstrasse 9, Munich, 80336, Germany

Received June 18, 2007; Revised Manuscript Received September 9, 2007

ABSTRACT: In order to gain a better understanding of the structure−function relation in hSGLT1, single Trp residues were introduced into a functional hSGLT1 mutant devoid of Trps at positions that previously had been postulated to be involved in sugar recognition/translocation and/or phlorizin binding. The mutant proteins were expressed in *Pichia pastoris*, purified, and reconstituted into liposomes. In transport experiments the putative sugar binding site mutants W457hSGLT1 and W460hSGLT1 showed a drastic decrease in affinity toward α-methyl-D-glucopyranoside with K_m values of 13.3 and 5.26 mM compared to 0.4 mM of the Trp-less hSGLT1. In addition, a strong decrease in the inhibitory effect of phlorizin was observed. In Trp fluorescence studies the position of the emission maxima of the mutants, their sensitivity to *N*-bromosuccinimide oxidation, and their interaction with water soluble quenchers demonstrate that Trp^{457} and Trp^{460} are in contact with the hydrophilic extravesicular environment. In both mutants Trp fluorescence was quenched significantly, but differently, by various glucose analogues. They also show significant protection by D-glucose and phlorizin against acrylamide, KI, or TCE quenching. W602hSGLT1 and W609hSGLT1, the putative aglucone binding site mutants, exhibit normal sugar and phlorizin affinity, and show fluorescence properties which indicate that these residues are located in a very hydrophilic environment. Phlorizin and phloretin, but not D-glucose, protect both mutants against collisional quenchers. Depth-calculations using the parallax method suggest a location of Trp^{457} and Trp^{460} at an average distance of 10.8 Å and 7.4 Å from the center of the bilayer, while Trp^{602} and Trp^{609} are located outside the membrane. These results suggest that in the native carrier residues Gln at position 457 and Thr at position 460 reside in a hydrophilic access pathway extending 5−7 Å into the membrane to which sugars as well as the sugar moiety of inhibitory glucosides bind. Residues Phe^{602} and Phe^{609} contribute by their hydrophobic aromatic residues toward binding of the aglucone part of phlorizin. Thereby in the phlorizin-carrier complex a close vicinity between these two subdomains of the transporter is established creating a phlorizin binding pocket with the previously estimated dimensions of 10 × 17 × 7 Å.

The life of every organism depends on the continuous supply of energy; one of the most important metabolic fuels is D-glucose. D-Glucose uptake into the cells requires transport proteins (*1*) and can be achieved either by passive diffusion via facilitating transporters of the GLUT family or by secondary active transport through sodium-glucose cotransporters (SGLTs) (*2*, *3*). SGLT1 accumulates D-glucose across the cell membrane against its concentration gradient by transforming the energy of the electrochemical Na^+-gradient into osmotic work. In humans, SGLT1 is involved in intestinal absorption and renal reabsorption of D-glucose and D-galactose.

The human isoform of SGLT1 (hSGLT1[1]) is 664 amino acids long with a predicted topology of 14 transmembrane helices and both the N- and C-terminus facing the extracellular fluid (*4*). Previous studies of hSGLT1 demonstrated that the N-terminal half of the protein contains the Na^+-binding sites (*5*), where Ala^{166} appears to be involved in Na^+ binding, while the sugar and inhibitor binding sites are located in the C-terminal half of the protein (*6*, *7*). Further molecular, biochemical, and biophysical studies indicated that residues Gln^{457}, Thr^{460} (*3*), and a negative charge at residue Asp^{454} form part of the sugar-binding and translocation pathway (*8*). The importance of Gln^{457} in sugar transport is

† This work was supported by funds of the International Max Planck Research School in Chemical Biology Dortmund, Germany (N.K.T.), the MPI Dortmund (A.K.), the August-Lenz-Stiftung and the Deutsche Forschungsgemeinschaft (Graduate Program "Vascular Biology in Medicine" GRK438 (P.G.), SFB 413 and Si 274/9).

* To whom correspondence should be addressed: Max Planck Institute of Molecular Physiology, Otto-Hahn-Str.11, Dortmund, 44227 Germany. Tel: 49-231-97426491. Fax: 49-231-97426479. E-mail: rolf.kinne@mpi-dortmund.mpg.de.

‡ Max Planck Institute of Molecular Physiology.

§ Present address: Department of Genetics and Howard Hughes Medical Institute, Yale University School of Medicine, New Haven, CT 06510.

|| Present address: National Institute on Aging, National Institutes of Health, 5600 Nathan Shock Drive, Baltimore, MD 21224.

⊥ Ludwig Maximilian University.

[1] Abbreviations: hSGLT1, human sodium/D-glucose cotransporter 1; D-Glc, D-glucose; Phlz, phlorizin; Phlo, phloretin; Trp, tryptophan; Phe, phenylalanine; KI, potassium iodide; TCE, trichloroethanol; K_{SV}, Stern−Volmer quenching constant.

10.1021/bi701193x CCC: $37.00
Published on Web 11/06/2007

also supported by the fact that mutation Q457R causes glucose-galactose-malabsorption by blocking sugar translocation (*9*). As reported for various sugar binding and transport proteins salt bridges also play a critical role in sugar binding and translocation (*10*−*12*). Indeed, mutational analysis of charged residues in the highly conserved transmembrane helices VII and VIII identified the negative charge of K^{321} as essential for the turnover rate and the cation selectivity of hSGLT1 uniport activity, and Na^+ and sugar binding during cotransporter activity (*13*).

Sodium-D-glucose cotransport is inhibited by glucosides with aromatic or aliphatic aglucone residues. Phlorizin, a β-glucoside of the aromatic compound phloretin, is the most effective inhibitor, with an apparent K_i of 1 μM (*14*). It is proposed that phlorizin binding to SGLT1 is a two-step process: rapid formation of an initial collision complex, followed by a slow isomerization process that occludes phlorizin within its receptor site (*15*). Phlorizin is thereby supposed to bind to both the sugar-binding site and an aglucone-binding site (*16*, *17*). The question which amino acids are critically involved in this process in the intact transporter is still a matter of debate. One study from our group (*18*) on rabbit SGLT1 expressed in CHO cells using site directed mutagenesis suggests that a hydrophobic region located in the C-terminal loop 13 (amino acid 604−610) is critically involved in the binding of phlorizin. However, a recent study from Gagnon et al. (*19*) on human SGLT1, using the substituted cysteine accessibility method in *Xenopus* oocytes, revealed that these amino acids appear not to be necessary for phlorizin binding to the carrier. Further support for the former assumption, that indeed a phlorizin binding site is located in this region, came from studies on isolated loop 13 of rabbit SGLT1 using fluorescence spectroscopy and affinity labeling (*20*, *21*). By using the same approach on isolated loop 13 of rabbit SGLT1 for another inhibitor of the sugar transporter, an alkyl-glucoside binding site was identified in between amino acids 601−630 (*22*).

Recently hSGLT1 could be expressed in and purified from *Pichia pastoris* in an active form (*23*). This allowed a closer look into the conformational geometry of the transporter. Intrinsic and extrinsic Trp fluorescence studies on the recombinant hSGLT1 identified three different conformational states of the transporter in solution (*23*) and in reconstituted proteoliposomes (*24*) confirming directly conclusions derived in previous kinetic and electrophysiological experiments (*25*, *26*). Furthermore the intramembrane arrangement of various Trps of the transporter could be determined (*24*). hSGLT1 contains 14 Trps residues at position 6, 45, 66, 67, 103, 114, 276, 289, 291, 440, 477, 487, 561, and 641. In a recent study (*27*) we mutated all Trp residues to Phe residues to create the Trp-less mutant W0hSGLT1; this mutant shows characteristic sodium-dependent, phlorizin-inhibitable transport properties and exhibits the same transport kinetics as wild type hSGLT1. Therefore, in the current study we used this mutant in mutagenesis, transport, and fluorescence studies to probe more precisely the components, environment, and location of the transporter domains involved in sugar recognition and phlorizin binding.

EXPERIMENTAL PROCEDURES

Materials. All sugars, phloretin, phlorizin, and trichloroethanol were from Sigma (Munich, Germany). All media (LB, YPD, BMMGY, and BMMY) were from Invitrogen (Carlsbad, CA). α-Methyl-D-[^{14}C] glucopyranoside ([^{14}C] α-MDG) was from Perkin-Elmer LAS (Rodgau-Jügesheim, Germany). Synthetic 1-palmitoyl-2-stearoyl (*n*-doxyl)-*sn*-glycero-3-phosphocholine (DoxylPC), with the spin labels at the 5- and 12-positions of the *sn*-2-acyl chain, was purchased from Avanti Polar Lipids Inc (Alabaster, AL). All other chemicals were of analytical grade and obtained from commercial sources.

Molecular Biology. A plasmid containing human hSGLT1 in Trps-less background named W0hSGLT1 (*27*) cDNA was used as a template for site directed mutagenesis studies. Four mutants of W0hSGLT1 containing single Trp residues at different positions (457, 460, 602, and 609) were generated by Quick-Change II site directed mutagenesis kit (Stratagene, La Jolla, CA) as per the manufacturer's instructions. The following oligonucleotides with mutated nucleotides (underlined) were used for mutagenesis. Q457W-sense, 5′-CTCTTCGATTACATCTGGTCCATCACCAG-3′; and antisense, 5′-CTGGTGATGGACCAGATGTAATCGAAGAG-3′; T460W-sense, 5′-ATCCAGTCCATCTGGAGTTACTTGGGACC-3′; and antisense, 5′-GGTCCCAAGTAACTCCAGATGGACTGGAT-3′; F602W-sense, 5′-AAAGGAATCTGGAGGAGAGCCTATGAC-3′; and antisense, 5′-GTCATAGGCTCTCCTCCAGATTCCTTT-3′, F609W-sense, 5′-GCCTATGACCTATGGTGTGGGCTAGAG-3′; and antisense, 5′-CTCTAGCCCACACCATAGGTCATAGGC-3′. All the constructs were confirmed by DNA sequencing (Agowa GmbH Berlin, Germany). For simplicity all mutants will be referred to only by the position of the Trp as W547, W460, W602, and W609hSGLT1.

Expression, Purification, and Reconstitution of Different hSGLT1 Mutants. Different mutants of hSGLT1 were expressed in *Pichia pastoris* and purified to homogeneity by nickel-affinity chromatography (*23*). Reconstitution of hSGLT1 mutants was performed into preformed Triton X-100-destablized liposomes composed of 90% (wt/vol) asolectin soy lecithin and 10% (wt/vol) cholesterol. The detergent-mediated solublization was followed by turbidity measurements (*28*). Detergent-destabilized liposomes were mixed with purified protein in a 150:1 (w/w) and incubated at room temperature under gentle agitation for 10 min. Detergent was removed by adding Bio-Beads SM-2 activated according to (*29*) at a wet weight beads:detergent ratio of 6:1. After 1 h of incubation at room temperature, fresh Bio-Beads were added, and incubation was continued for an additional hour. After the third addition of Bio-Beads, incubation was continued overnight at 4 °C. Bio-Beads were removed by filtration on glass silk. Proteoliposomes were concentrated by centrifugation at 300000*g* for 45 min at 4 °C and stored in liquid nitrogen.

Analytical Methods. Coomassie Blue staining was performed after protein separation by SDS−PAGE using 10% acrylamide gels as described (*23*). Western blot analysis of gel separated proteins was performed by using murine cell culture anti-FLAG M2 monoclonal antibody peroxidase conjugate (Sigma, Munich, Germany).

Transport Studies. Proteoliposomes (preloaded with 100 mM potassium phosphate, pH 7.5/2 mM β-mercaptoethanol)

were subjected to three sonication/freeze/thaw cycles before uptake assays at 22 °C. Uptake was initiated by mixing 10 μL of proteoliposomes with 10 μL of transport buffer 2X (200 mM choline/Cl, 50 mM NaCl, 100 mM mannitol, 20 mM Tris, 20 mM HEPES, 6 mM $MgSO_4$, 2 mM $CaCl_2$) with α-methyl-D-[^{14}C] glucopyranoside ([^{14}C] α-MDG). Each reaction was stopped by the addition of 1 mL of ice-cold stop solution (10 mM Tris, 10 mM HEPES, 100 mM mannitol, 150 mM KCl, 50 mM choline/Cl, 50 mM NaCl, 3 mM $MgSO_4$, 1 mM $CaCl_2$, 0.2 mM phlorizin). The proteoliposomes were applied centrally to a 0.22 μm nitrocellulose filter GSWP (Millipore) over vacuum, washed with 3 mL of ice-cold stop solution, and the filter was assayed by scintillation counting. All experiments were performed at least in triplicate.

For the determination of K_m the rate of uptake *versus* substrate concentration curves were fitted to the Michaelis−Menten equation, $v/V_{max} = [S]/([S] + K_m)$, using a nonlinear regression analysis in Origin program (OriginLab, Northampton, MA).

Steady-State Fluorescence Studies and Ligand Binding Assay. All fluorescence experiments reported in this study were performed with W457hSGLT1, W460hSGLT1, W602hSGLT1, or W609hSGLT1 reconstituted into proteoliposomes (liposomes were composed of 9:1 asolectin soy lecithin and cholesterol). The final protein concentration was 5 μM, and the lipid/protein molar ratio was 150:1. Steady-state fluorescence measurements were done with a LS 50B fluorescence spectrometer (Perkin-Elmer), fitted with a 450 W xenon arc lamp at room temperature. A 0.3-cm excitation and emission path length quartz cell was used for all the fluorescence measurements. The excitation wavelength was set at 295 nm for selective excitation of Trp. A 290 nm cutoff filter was used to minimize the contribution of scattering signals. Emission spectra were collected from 310 to 380 nm, averaging six scans. The bandwidths for both excitation and emission monochromators were 5 nm. The emission spectra were corrected for the liposome blank (scattering), dilution effects, and inner-filter effects, which at the maximal lipid concentration used contributed at most 10% to the total signal. The ligand-induced fluorescence change as a function of ligand concentration was monitored as described previously (*23*). Apparent binding constants for ligands were calculated by the equation

$$\Delta F/\Delta F_{max} = [S]/[S] + K_d$$

where [S] is the external substrate concentration, ΔF_{max} is the maximal change in fluorescence intensity for saturating [S], and K_d is dissociation constant.

Quenching of Intrinsic Protein Fluorescence by Collisional Quenchers. Steady-state fluorescence quenching was carried out by measuring the fluorescence intensities at the emission maxima as a function of the quencher concentrations. Increasing concentrations of the quenchers were added from a concentrated stock solution of the quenchers in the same buffer. All quencher solutions were freshly prepared, and 0.1 mM $Na_2S_2O_3$ was added to the KI stock solution to prevent I_3^- formation. The accessibility of Trp was monitored by analyzing the quenching data using a Stern−Volmer equation,

$$F_0/F = 1 + K_{SV}[Q]$$

where F_0 and F are the fluorescence intensities in the absence and presence of quencher, respectively, [Q] is the concentration of quenching agent, and K_{SV} is the Stern−Volmer quenching constant. In the case of a purely collisional quenching mechanism, a Stern−Volmer plot of F_0/F *versus* [Q] gives a linear plot with a slope value equal to K_{SV}.

Measurements of Intramembrane Location of Trp Residues in Mutants Reconstituted in Liposomes Using the Parallax Method. Average depth of Trp residue in different hSGLT1 mutants reconstituted into POPC liposomes was calculated by the parallax method (*30*, *31*) using the equation

$$z_{cF} = L_{c1} + \{[(-1/\pi C)\ln(F_1/F_2) - L_{21}^2]/2L_{21}\}$$

where z_{cF} = the depth of the fluorophore from the center of the bilayer, L_{c1} = the distance of the center of the bilayer from the shallow quencher (5-Doxyl PC in our case), L_{21} = the difference in depth between the two quenchers, and C = the 2-dimensional quencher concentration in the plane of the membrane (molecule/Å^2). Here F_1/F_2 is the ratio of the F_1/F_0 and F_2/F_0 in which F_1 and F_2 are fluorescence intensities in the presence of the shallow (5-Doxyl PC) and deep quencher (12-Doxyl PC) respectively, both at the same quencher concentration C; F_0 is the fluorescence intensity in the absence of any quencher. All the bilayer parameters used were the same as described previously (*24*, *30*, *31*).

N-Bromosuccinimide Modification of Different Mutants of hSGLT1 in Proteoliposomes. W457, 460, 602, and 609 hSGLT1 mutants (5 μM) reconstituted in liposomes were subjected to NBS modification by a 5-fold molar excess of NBS over the protein, using 2 mM stock solution of NBS in the same buffer (*24*). The fluorescence intensity at 340−350 nm (depending on the fluorescence emission maximum of the mutant) was monitored at an excitation wavelength of 295 nm. In each case the fluorescence intensity of the same amount of mutant protein without NBS modification was used as control.

RESULTS

Protein Purification. W457hSGLT1, W460hSGLT1, W602hSGLT1, and W609hSGLT1 were expressed in *Pichia pastoris* and purified to homogeneity with a yield of ∼1.5, 1.8, 2.1, and 2.5 mg/L culture, respectively. Proteins were more than 95% pure as judged by Coomassie staining and Western blot analysis with anti-FLAG antibody (Figure 1).

Transport Properties of Proteoliposomes Containing W457hSGLT1, W460hSGLT1, W602hSGLT1, and W609hSGLT1. As shown in Figure 2 and Table 1, in proteoliposomes made of hSGLT1, α-MDG uptake in the presence of a sodium gradient reached 1874 ± 55 nmol × mg of hSGLT1^{-1} × min^{-1}, and the uptake was almost completely blocked by phlorizin (301 ± 60 nmol × mg of hSGLT1^{-1} × min^{-1}). When Gln^{457} was mutated into Trp^{457}, an 80% decrease in α-MDG uptake in the presence of sodium (375 ± 21 nmol × mg of W457hSGLT1^{-1} × min^{-1}) was observed, and inhibition by phlorizin amounted only to 20%. In mutant W460hSGLT1 which is devoid of Thr^{460}, α-MDG uptake decreased by 66%; again phlorizin was less effective. Mutant W602hSGLT1 (Phe^{602} → Trp^{602}) and W609hSGLT1 (Phe^{609} → Trp^{609}) show almost the same α-MDG uptake as the

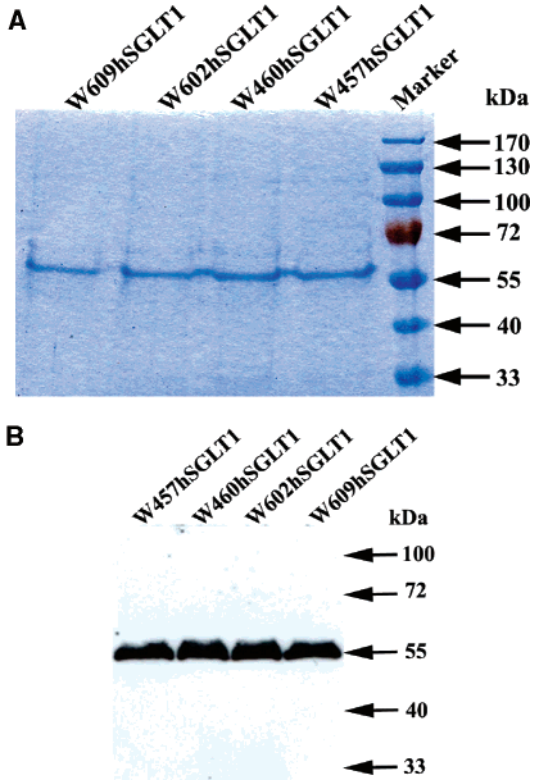

FIGURE 1: Coomassie-stained SDS−PAGE gel and immunoblot of it with anti-FLAG antibody of purified W457hSGLT1, W460hSGLT1, W602hSGLT1, and W609hSGLT1.

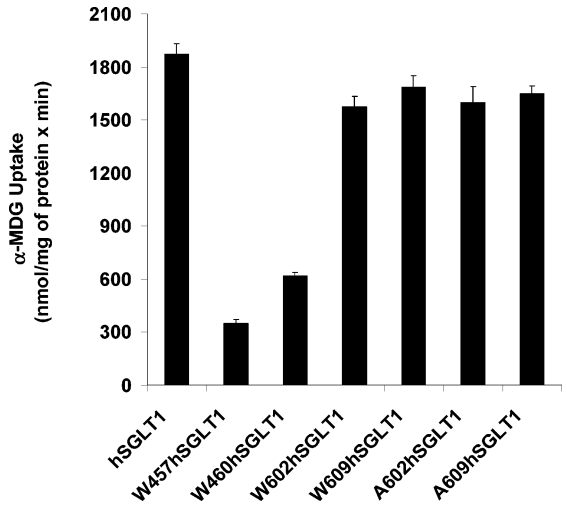

FIGURE 2: Sugar uptake characteristics of proteoliposomes containing purified recombinant hSGLT1, W457hSGLT1, W460hSGLT1, W602hSGLT1, W609hSGLT1, A602hSGLT1, or A609hSGLT1 proteins. 50 μM α-MDG uptake by proteoliposomes made of purified hSGLT1, W457hSGLT1, W460hSGLT1, W602hSGLT1, W609hSGLT1, A602hSGLT1, and A609hSGLT1 transport 1874 ± 55, 375 ± 21, 644 ± 25, 1648 ± 58, 1685 ± 64, 1598 ± 88, and 1650 ± 41 nmol × mg of protein^{-1} × min^{-1}, respectively, in the presence of 100 mM Na^+ and 50 μM α-MDG. Sugar transport for each mutant in different conditions is compiled in Table 1. The mean ± SD of three independent experiments is given.

control (Table 1), and no effect on the inhibitory potential of phlorizin is evident.

Apparent transport affinities of different sugars for the recombinant wild type hSGLT1 and the mutants are compiled in Table 2. The D-glucose K_m for hSGLT1 was 0.51 mM, but 1DOglc had a 22-fold lower affinity for the transporter

Table 1: Sugar Uptake by Proteoliposomes Containing hSGLT1 or Its Mutants in Different Conditions[a]

protein	α-MDG uptake (nmol/mg of protein × min)		inhibition of sugar uptake by phlorizin (% of control)
	sodium (control)	sodium + Phlz	
hSGLT1	1874 ± 55	301 ± 60	84
W457hSGLT1	375 ± 21	295 ± 34	22
W460hSGLT1	644 ± 25	480 ± 46	26
W602hSGLT1	1648 ± 58	342 ± 25	80
W609hSGLT1	1685 ± 64	294 ± 41	83
A602hSGLT1	1598 ± 88	1480 ± 60	8
A609hSGLT1	1650 ± 41	1539 ± 50	7

[a] Uptake experiments were performed in the presence of 50 μM α-MDG, 100 mM Na^+, and 100 μM phlorizin. The same concentrations of phospholipids were used in all experiments.

with a K_m of 11.2 mM, indicating the importance of an −OH group at the C1 position of the sugar. The K_m for α-MDG (containing a methyl group in equatorial orientation at the C1 position) was 0.4 mM (Figure 3). As expected, the most dramatic change in affinity occurred when the sugar lost its equatorial −OH at the C2 position, and the K_m for 2DOglc was >100 mM, since this equatorial −OH group plays a major role in sugar recognition by the transporter. 3OMglc had a K_m of 7.7 mM. The only increase in apparent affinity, as compared with D-glucose, was found when the equatorial −OH group at the C4 position was replaced with a stronger hydrogen bond acceptor −F (4F4DOglc) with a K_m of 0.06 mM. Changing the orientation of the C4 −OH group from equatorial to axial in D-galactose had no effect on its affinity toward the transporter. Replacing the pyranose O with S in the ring of the sugar, as in 5Thioglc, increased the K_m to 4.4 mM. The apparent affinity for 6DOglc was determined to be 3.2 mM. L-glucose, which is a nontransported sugar, does not interact with transporter. Phlorizin was the most potent competitive inhibitor of sugar transport with an inhibition constant of 5 μM (Table 2).

For mutant W457hSGLT1 (Figure 3 and Table 2) the α-MDG affinity decreased 33-fold as compared to the wild type hSGLT1 from a K_m value of 0.4 mM (hSGLT1) to 13.3 mM. Other sugars also showed a similar trend in their respective affinities toward this mutant. This mutant also shows less inhibition by phlorizin on sugar transport as compared to the wild type transporter, with an inhibition constant of 20 μM, which is 4-fold higher than the value determined for hSGLT1 (5 μM).

In W460hSGLT1 (Figure 3 and Table 2) α-MDG affinity was 13 times lower than in hSGLT1 (5.26 *versus* 0.4 mM). Similarly the affinity to other sugars was reduced. This mutant also shows a 3-fold decrease in its affinity toward phlorizin, with a value of 15 μM. However, phloretin, the aglucone moiety of phlorizin, exhibits affinities toward both mutants comparable to those of the wild type transporter. The importance of residues Gln^{457} and Thr^{460} on sugar transport were further signified by the lower maximum velocity (V_{max}) values (Figure 3). hSGLT1 shows a V_{max} of 3.4 ± 0.34 μmol × mg protein^{-1} × min^{-1}, while mutant W457hSGLT1 and W460hSGLT1 give a V_{max} of 1.3 ± 0.05 and 1.6 ± 0.06 μmol × mg protein^{-1} × min^{-1}, respectively.

On the contrary, W602hSGLT1 and W609SGLT1 show apparent transport affinities for sugars that are very similar

Table 2: Summary of Apparent Affinities for Each Sugar in hSGLT1, W457hSGLT1, W460hSGLT1, W602hSGLT1, and W609hSGLT1

		K_m (mM)				
ligands	changes[a]	hSGLT1	W457hSGLT1	W460hSGLT1	W602hSGLT1	W609hSGLT1
D-Glc	no	0.51 ± 0.02	14.7 ± 1.5	5.97 ± 0.8	0.52 ± 0.02	0.51 ± 0.01
α-MDG	−CH_3 group at C-1	0.40 ± 0.05	13.3 ± 1.2	5.26 ± 0.06	0.47 ± 0.03	0.46 ± 0.02
1DOglc	no −OH group at C-1	11.2 ± 1.5	60.5 ± 4.5	nd[b]	12.5 ± 1.1	11.8 ± 1.3
2DOglc	no −OH group at C-2	>100	nd	nd	>100	>100
3OMglc	−CH_3 group at C-3	7.7 ± 1.8	128.5 ± 14.8	65.3 ± 7.5	8.0 ± 1.6	7.5 ± 1.0
D-Gal	axial OH group at C-4	0.56 ± 0.03	15.9 ± 0.8	6.5 ± 1.1	0.57 ± 0.05	0.58 ± 0.04
4F4DOglc	−F group at C-4	0.06 ± 0.01	0.45 ± 0.01	0.33 ± 0.02	0.28 ± 0.01	0.31 ± 0.02
5Thioglc	−S group in pyranose ring	4.4 ± 0.8	35.7 ± 3.8	nd	4.3 ± 1.0	4.4 ± 1.5
6DOglc	no −OH group at C-6	3.2 ± 0.5	4.5 ± 0.04	4.1 ± 0.05	3.6 ± 0.07	3.3 ± 0.05
Phlz (K_i)	phloretin moiety at C-1	0.005 ± 0.0008	0.020 ± 0.001	0.015 ± 0.0009	0.005 ± 0.0007	0.005 ± 0.0008
L-Glc	L-isomer of glucose	na[c]	na	na	na	na

[a] All changes are with respect to D-glucose. [b] Not detected. [c] Not applicable.

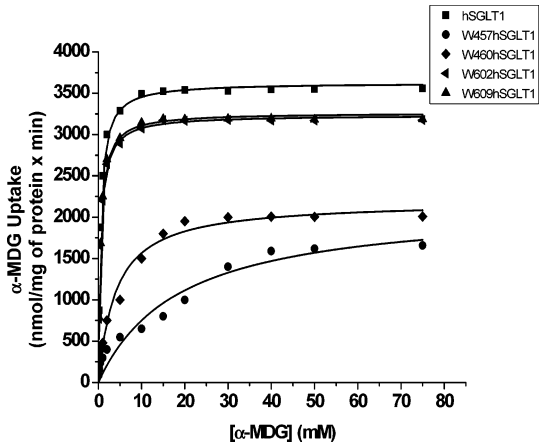

FIGURE 3: Sugar uptake kinetics of proteoliposomes containing purified recombinant hSGLT1, W457hSGLT1, W460hSGLT1, W602hSGLT1, and W609hSGLT1 proteins. Concentration dependence of the sugar uptake after 1 min shows K_m values of 0.4 ± 0.05, 13.3 ± 1.2, 5.26 ± 0.06, 0.47 ± 0.03, 0.46 ± 0.02 mM and maximum velocity (V_{max}) of 3.4 ± 0.34, 1.3 ± 0.05, 1.6 ± 0.06, 3.1 ± 0.21, 3.2 ± 0.30 μmol × mg protein^{-1} × min^{-1} for hSGLT1 (■), W457hSGLT1 (●), W460hSGLT1 (▲), W602hSGLT1 (▼), and W609hSGLT1 (left-facing solid triangle), respectively. Data points (shown by symbols) were fitted to the Michaelis−Menten equation, as shown by solid line, and the values of K_m were determined in the Origin program. All data fitted well in Michaelis−Menten equation with $R^2 = 0.95$ indicating the high quality fit of the nonlinear regression line with the data points.

to those determined for hSGLT1 (Figure 3 and Table 2). They also exhibit normal inhibitory effects of phlorizin on sugar transport, with the same inhibition constants as for the wild type transporter. Mutant W602hSGLT1 and W609hSGLT1 also show only a small decrease in V_{max} (Figure 3).

Fluorescence Properties of Mutants. Trp fluorescence has been used systematically as an internal reporter to study location, environment, and conformational changes in proteins after interaction with ligands and inhibitors. It is well-known that the emission properties of the indole ring are very sensitive to changes in microenvironment. W457hSGLT1 and W460hSGLT1 exhibit emission maxima at 343 and 340 nm, respectively (Figure 4A and B), showing that the indole ring lies in a moderately hydrophilic environment. This finding is quite surprising as these residues are present in transmembrane domain XI predicted to be buried inside the membrane (*4*), but this phenomenon has been observed also for a few other membrane proteins (*32*). The corrected emission spectra of W602hSGLT1 and W609hSGLT1 are shown in Figure 4 (C and D, respectively). The emission maxima of both Trp mutants are in the range of 346−350 nm, which is typical for a very hydrophilic environment. The position of the emission maxima for these two mutants fits very well with the predicted location of these residues in the extramembranous loop 13 of the transporter.

The effect of different sugars and inhibitors on Trp fluorescence of each mutant is compiled in Table 3A and B. D-Glucose quenches Trp fluorescence of mutants W457hSGLT1 and W460hSGLT1 by 57% and 36%, respectively; while phlorizin does so by 50% and 31%. It is worth mentioning that in the presence of D-glucose or phlorizin, mutant W457hSGLT1 does not show any shift in emission maxima, while mutant W460hSGLT1 shows a 3−4 nm blue shift. The mutants also differ with regard to the quenching of their intrinsic fluorescence by different sugars. Thus 5-thioglucose quenches W457hSGLT1 to the highest extent whereas the quenching of W460hSGLT1 is most sensitive to 4−fluor-4-deoxy-D-glucose. In order to distinguish which part of phlorizin, the sugar moiety or aglucone part, is responsible for fluorescence quenching, we recorded Trp fluorescence of both mutants in the presence of 100 μM phloretin. A much lower quenching in Trp fluorescence was found for both mutants (5% for mutant W457hSGLT1 and 6% for mutant W460hSGLT1). As expected, in the presence of L-glucose both mutants do not show any change in fluorescence (Table 3A). These results indicate that residues located in position 457 and 460 are involved, although probably in a different manner, in sugar recognition/translocation and provide also a binding site for the sugar moiety of phlorizin.

In mutants W602hSGLT1 and W609hSGLT1, 10 mM D-glucose increased the Trp fluorescence by 11% and 14% without any shift in emission maxima (Figure 4C and D). When Trp fluorescence experiments were performed in the presence of 100 μM phlorizin or phloretin, fluorescence decreased by 80% and 84% for W602hSGLT1 and W609hSGLT1 with 5−6 nm red shifts in emission maxima. These results support the notion that residues Phe^{602} and Phe^{609} interact with the aglucone part of phlorizin, phloretin.

The K_d values obtained in the fluorescence titration experiments are in general in good agreement with the relative affinities (K_m values) of these compounds as assessed by transport kinetics (Table 2). For example the K_d values for D-glucose for mutant W457hSGLT1 and W460hSGLT1 are 15.1 mM and 6.5 mM respectively; these values are 18- and 8-fold lower than values determined for hSGLT1 (0.84 mM, Table 3A). Most interestingly, again the K_d values for

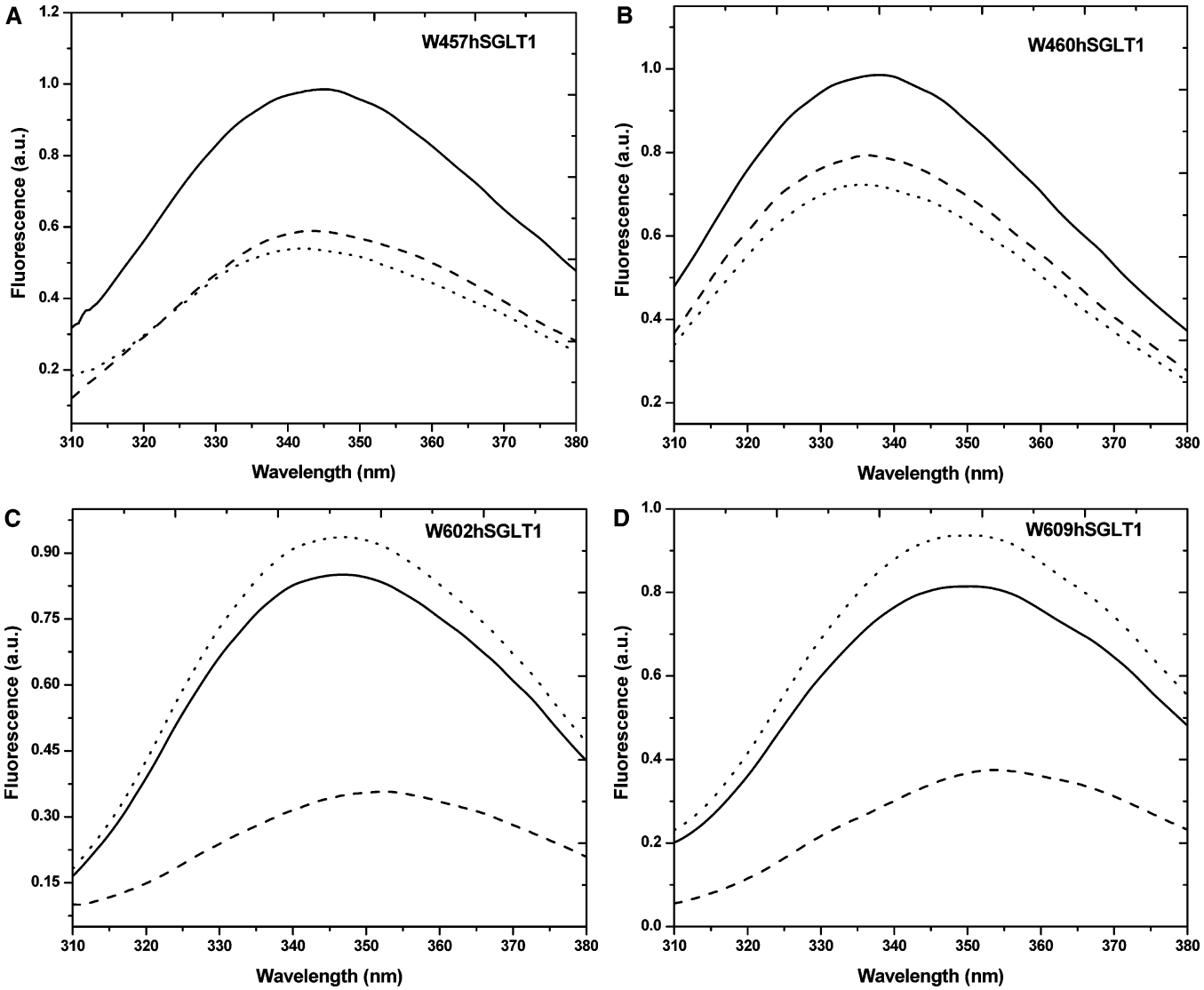

FIGURE 4: Effect of D-glucose or phlorizin on the corrected emission spectrum of (A) W457hSGLT1, (B) W460hSGLT1, (C) W602hSGLT1, and (D) W609hSGLT1. For each experiment, 5 μM protein reconstituted into proteoliposomes in the ratio of 150:1 was incubated in the absence (solid line), presence of 10 mM D-glucose (dotted line), or presence of 100 μM phlorizin (dashed line). The excitation wavelength was 295 nm. The results shown are typical of ≈20 independent experiments. All of the spectra were corrected as described in Experimental Procedures; a.u., arbitrary units.

phlorizin for W457hSGLT1 and W460hSGLT1 were 25 μM and 17 μM, respectively; these values indicate that phlorizin binding with both mutants is 5- and 3-fold weaker than in the wild type transporter. However, for saturating concentration of phloretin both mutants show less fluorescence quenching than hSGLT1 but their K_d values are comparable (Table 3A). Changes in the K_d values for other ligands for both mutants follow the same trend as previously seen in transport studies (Table 2). The intense effects on the K_d values for sugars and phlorizin due to replacement of Gln at position 457 and Thr at position 460 by Trps clearly underline the importance of these residues in sugar binding and providing binding sites for the sugar moiety of phlorizin.

For mutants W602hSGLT1 and W609hSGLT1 the K_d values for different sugars and inhibitors exactly mirror the values obtained for hSGLT1 (Table 3A and B). The extent of quenching or increase induced by saturating concentrations of various ligands did not uniformly appear to correlate with the affinity of the ligands for binding to different mutants. For example, in mutant W457hSGLT1 low-affinity substrate 5-thioglucose (K_d = 39.1 mM) induced a maximum quenching of ~75%, while high-affinity substrate D-glucose (K_d = 15.1 mM) and high-affinity inhibitor phlorizin (K_d = 25 μM) quench only 57% and 50% Trp fluorescence. Saturating concentration of phloretin quenches 20% Trp fluorescence of hSGLT1, 5% of W457hSGLT1, and 6% of W460hSGLT1 fluorescence, but its K_d values remains unaltered for all three proteins. For mutants W602hSGLT1 and W609hSGLT1 saturating concentrations of phlorizin and phloretin quench Trp fluorescence up to equal extents (Table 3B) but their binding affinities differ by at least 8-fold. These discrepancies are most probably due to the different nature of K_d and K_m values. K_d values represent binding constants obtained under equilibrium conditions whereas K_m values represent apparent affinities of the complex overall translocation process.

Trp Fluorescence Quenching of Mutants by Acrylamide, KI, and TCE in the Presence and Absence of D-Glucose or Phlorizin. The quenching of Trp fluorescence for different mutants of hSGLT1 in the absence and presence of substrates and inhibitors using water-soluble quenchers (acrylamide,

Table 3: Binding Affinity of Different Ligands with hSGLT1 and Its Different Mutants as Determined by Change in Intrinsic Fluorescence[a]

A. hSGLT1, W457hSGLT1, and W460hSGLT1

	hSGLT1		W457hSGLT1		W460hSGLT1	
ligands	ΔF (%)	K_d[b] (mM)	ΔF (%)	K_d[b] (mM)	ΔF (%)	K_d[b] (mM)
D-Glc	+13.0 ± 1.0	0.84 ± 0.15	−57.0 ± 6.3	15.1 ± 1.2	−36.5 ± 4.0	6.5 ± 1.2
α-MDG	+15.0 ± 3.5	0.71 ± 0.10	−58.1 ± 4.7	12.0 ± 0.98	−37.0 ± 3.5	6.1 ± 0.5
1DOglc	+1.1 ± 0.2	14.3 ± 2.5	−10.3 ± 1.2	65.7 ± 3.5	no	no
2DOglc	no	no	no	no	no	no
3OMglc	+2.6 ± 0.5	8.1 ± 0.97	−5.9 ± 1.0	119.9 ± 10.3	−3.0 ± 0.2	75.1 ± 8.3
D-Gal	+12.0 ± 2.3	0.86 ± 0.11	−57.2 ± 5.0	15.8 ± 1.1	−36.9 ± 3.9	7.5 ± 1.4
4F4DOglc	+25.0 ± 4.2	0.15 ± 0.03	−65.0 ± 4.5	0.51 ± 0.02	−86.3 ± 3.9	0.30 ± 0.04
5Thioglc	+6.5 ± 0.4	4.9 ± 1.3	−75.0 ± 2.0	39.1 ± 2.6	−5.0 ± 1.0	no
6DOglc	+7.3 ± 1.0	3.7 ± 0.79	−10.8 ± 1.7	4.9 ± 0.7	−12.0 ± 1.0	4.5 ± 0.4
Phlz	−50.0 ± 5.0	0.005 ± 0.0005	−50.1 ± 4.5	0.025 ± 0.003	−31.0 ± 3.0	0.017 ± 0.001
Phlo	−20.0 ± 3.0	0.045 ± 0.007	−5.0 ± 0.7	0.043 ± 0.003	−6.0 ± 1.0	0.041 ± 0.003
L-Glc	no	no	no	no	no	no

B. W602hSGLT1 and W609hSGLT1

	W602hSGLT1		W609hSGLT1	
ligands	ΔF (%)	K_d[b] (mM)	ΔF (%)	K_d[b] (mM)
D-Glc	+11.3 ± 1.2	0.89 ± 0.05	+14.1 ± 2.0	0.72 ± 0.04
α-MDG	+11.9 ± 1.0	0.083 ± 0.03	+16.3 ± 2.0	0.66 ± 0.02
1DOglc	no	no	no	no
2DOglc	no	no	no	no
3OMglc	no	no	no	no
D-Gal	+10.0 ± 1.2	0.85 ± 0.07	+13.4 ± 1.5	0.75 ± 0.01
4F4DOglc	+13.0 ± 2.0	0.12 ± 0.01	+18.5 ± 2.5	0.10 ± 0.01
5Thioglc	no	no	no	no
6DOglc	+2.0 ± 0.2	no	+1.5 ± 0.1	no
Phlz	−80.1 ± 10.0	0.0045 ± 0.0011	−84.3 ± 11.7	0.0041 ± 0.0009
Phlo	−80.0 ± 12.9	0.040 ± 0.006	−83.3 ± 13.9	0.034 ± 0.008
L-Glc	no	no	no	no

[a] Plus sign (+)/minus sign (−) indicate increase/decrease in the fluorescence intensity after addition of ligand. [b] The apparent equilibrium dissociation constant (K_d) was determined from the nonlinear regression analysis of the percentage of fluorescence increase or decrease as a function of ligand concentration using a computer-based analysis program (Origin). Values are the means ± SD of three independent experiments.

Table 4: Stern−Volmer Quenching Constants (K_{SV}) of hSGLT1, W457hSGLT1, W460hSGLT1, W602hSGLT1, and W609hSGLT1 Reconstituted into Proteoliposomes in Different Conditions

	K_{SV}[e] (M^{-1})			
mutants	in the absence of ligand[a]	in the presence of 10 mM D-glucose[b]	in the presence of 100 μM phlorizin[c]	in the presence of 100 μM phloretin[d]
		A. Acrylamide		
W457hSGLT1	2.03 ± 0.03	0.76 ± 0.01	1.13 ± 0.01	2.16 ± 0.02
W460hSGLT1	1.74 ± 0.02	0.46 ± 0.01	1.02 ± 0.02	1.83 ± 0.02
W602hSGLT1	3.95 ± 0.08	3.45 ± 0.09	1.17 ± 0.03	2.03 ± 0.01
W609hSGLT1	4.02 ± 0.07	3.63 ± 0.07	1.20 ± 0.02	1.58 ± 0.03
		B. KI		
W457hSGLT1	1.08 ± 0.02	0.59 ± 0.02	0.79 ± 0.03	1.16 ± 0.02
W460hSGLT1	0.72 ± 0.01	0.34 ± 0.01	0.50 ± 0.01	0.85 ± 0.05
W602hSGLT1	2.71 ± 0.04	2.52 ± 0.06	1.09 ± 0.03	1.47 ± 0.03
W609hSGLT1	2.90 ± 0.03	2.49 ± 0.04	0.98 ± 0.02	1.55 ± 0.05
		C. TCE		
W457hSGLT1	2.88 ± 0.02	0.88 ± 0.02	1.21 ± 0.01	2.95 ± 0.05
W460hSGLT1	1.95 ± 0.02	0.52 ± 0.01	1.13 ± 0.03	2.05 ± 0.02
W602hSGLT1	4.69 ± 0.09	4.36 ± 0.06	1.39 ± 0.02	2.03 ± 0.06
W609hSGLT1	5.66 ± 0.07	5.32 ± 0.07	1.69 ± 0.04	2.23 ± 0.05

[a] Quenching experiments were conducted in the absence of ligand. [b] Quenching experiments were conducted in the presence of 10 mM D-glucose. [c] Quenching experiments were conducted in the presence of 100 μM phlorizin. [d] Quenching experiments were conducted in the presence of 100 μM phloretin. [e] The Stern−Volmer quenching constants were determined from the slopes of the lines of $F_0/F = 1 + K_{SV}[Q]$. Values are the mean ± SD of three independent experiments.

iodide, or TCE) provides further means to examine the environment and functional role of the Trp residues. All experimental data fitted linear Stern−Volmer plots for collisional (dynamic) quenching, thereby excluding a contribution from static quenching. The Stern−Volmer constants for all mutants are compiled in Table 4. Mutants W457hSGLT1 and W460hSGLT1 show moderate quenching by acrylamide with K_{SV} values of 2.03 M^{-1} and 1.74 M^{-1} (Table 4A). In the presence of D-glucose and phlorizin both mutants show a drastic decrease in quenching with much smaller K_{SV} values (Table 4A). On the contrary, in the presence of phloretin, which lacks the sugar moiety of phlorizin, both mutants show

Table 5: NBS Oxidation of Different hSGLT1 Mutants Reconstituted into Proteoliposomes

	residual fluorescence (%)			
conditions	W457hSGLT1	W460hSGLT1	W602hSGLT1	W609hSGLT1
no NBS	100	100	100	100
NBS	0	0	0	0
D-Glc + NBS[a]	91	88	0	0
L-Glc +NBS[b]	0	0	0	0
Phlz + NBS[c]	88	75	71	65
Phlo + NBS[d]	0	0	62	55

[a] NBS modification experiments were carried in the presence of 10 mM D-glucose. [b] NBS modification experiments were carried out in the presence of L-glucose. [c] NBS modification experiments were carried out in the presence of 100 μM phlorizin. [d] NBS modification experiments were carried in the presence of 100 μM phloretin.

higher K_{SV} values than in the absence of ligands (Table 4A). The higher K_{SV} values might indicate conformational changes in other parts of the transporter that make Trp^{457} and Trp^{460} more accessible for acrylamide.

The much higher K_{SV} values for acrylamide quenching obtained for mutants W602hSGLT1 and W609hSGLT1 point to a very high degree of solvent exposure for Trp^{602} and Trp^{609} (Table 4A). Importantly, there are significant reductions in K_{SV} values for mutants W602hSGLT1 and W609hSGLT1 in the presence of phlorizin (70% less quenching) and phloretin (48% and 54% less quenching for Trp^{602} and Trp^{609}). Mutants W602hSGLT1 and W609hSGLT1 show, however, only 10−12% less quenching in the presence of D-glucose. In the presence of L-glucose (data not shown) no reduction in the K_{SV} values for all four mutants was observed.

To provide further information on polarity and charge of the region surrounding the fluorophore, we used also KI and trichloroethanol. The K_{SV} values for all four mutants for KI were less as compared to acrylamide or TCE probably due to the charged nature of this quencher as Trps in all mutants have a negatively charged amino acid nearby. TCE, which is neutral and a less polar quencher than acrylamide, shows the highest K_{SV} values for all four proteins, indicating that the Trp residues are located in an environment which also contains some hydrophobic elements.

N-Bromosuccinimide Oxidation of Different Mutants Reconstituted into Proteoliposomes in the Presence and Absence of D-Glucose or Phlorizin. Since the fluorescence emission maxima and fluorescence quenching studies of the four mutants of hSGLT1 suggested that the Trps are located in recognition sites with accessibility from the extravesicular space, we performed NBS oxidation studies of the Trp mutants in the presence and absence of D-glucose and inhibitors. In the presence of a 5-fold molar excess of NBS over transporter protein, Trp fluorescence of all mutants was completely quenched within 1 min after NBS addition (Table 5). Furthermore, Trp^{457} and Trp^{460} in mutant W457hSGLT1 and W460hSGLT1 were almost completely protected against NBS modification by saturating concentrations of D-glucose or phlorizin (Table 5). However, phloretin or L-glucose did not provide any protection against NBS modification. On the contrary, in mutants W602hSGLT1 and W609hSGLT1, saturating concentrations of phlorizin or phloretin provided the same protection against modification by NBS (Table 5), but no protection by D-glucose was observed. These results further support the notion that the area around amino acids 457 and 460 is part of the D-glucose recognition/translocation pathway and provides a binding site for the sugar moiety of phlorizin as well. On the other hand, positions near amino acids 602 and 609 form part of the binding sites for phloretin, the aglucone moiety of phlorizin.

To confirm that the different transporter mutants were reconstituted in the proteoliposomes in one orientation, we constructed the single Trp mutant of hSGLT1, W66hSGLT1. Based on topology models of hSGLT1, this Trp residue is present on the membrane face opposite to Trp 457 or 460. When we performed NBS oxidation of the Trp residue of W66hSGLT1 reconstituted into liposomes, we did not get any significant fluorescence quenching. This indicates that Trp 66 is not accessible for NBS modification due to its different position within the transporter and location in the proteoliposomes. However, in solution or in proteoliposomes treated by 4 mM CHAPS detergent, this Trp is completely oxidized by 5-fold molar excess of NBS within 1 min. This result clearly indicates that, on the one hand, NBS, at least in the current experimental setup, does not penetrate the membrane and, on the other hand, all proteins were reconstituted in one orientation in the membrane. These results support the view that all mutants investigated in this study, when incorporated into proteoliposomes, assume only one orientation within the membrane (see Discussion for further evidence).

As reported in the literature NBS can brominate unsaturated lipids (*33*) and break down the lipid bilayer. To test the possibility that proteoliposomes in the current experimental design are not stable after treatment with NBS, we performed calcein release assays from proteoliposomes containing mutant protein after NBS treatment. 25 or 250 μM NBS treatment of proteoliposomes filled with calcein dye did not yield any increase in calcein fluorescence even after incubation for 1 h after NBS treatment. Detergent treatment of calcein containing proteoliposomes lead instantaneous increase in calcein fluorescence. Those results clearly indicate that proteoliposomes are stable after treatment with NBS even at a 10-fold higher concentration than that used for the fluorescence experiments.

Membrane Penetration Depth of Mutant Trps in Reconstituted Liposomes. To gain further and more precise insight into the membrane localization of the Trp residues in the different hSGLT1 mutants, average penetration depths of the Trp residues were determined by the parallax method. To this end we studied quenching of the Trp fluorescence for the four mutants reconstituted into POPC liposomes containing 5-Doxyl PC or 12-Doxyl PC. The average depths of penetration of the Trp residue determined for the different hSGLT1 mutants are compiled in Table 6. The Trp residue in the W457hSGLT1 protein is, on the average, positioned at a relatively shallow location in the membrane as evidenced

Table 6: Depth-Calculation of Trp Residue Locations in hSGLT1 Mutants Reconstituted into Liposomes (Parallax Method)[a]

mutant	F_5/F_0	F_{12}/F_0	F_5/F_{12}	distance of Trp from the bilayer center (Å)
W457hSGLT1	0.75 ± 0.08	0.71 ± 0.03	1.05	10.8 ± 0.5
W460hSGLT1	0.56 ± 0.01	0.78 ± 0.05	0.72	7.4 ± 0.3

[a] F_5 and F_{12} Trp fluorescence intensity in POPC-containing vesicles containing 5-Doxyl PC or 12-Doxyl PC quenchers in 15 mol %.

from the average distance of 10.8 Å from the center of the bilayer. This value is consistent with an interfacial localization of the Trp residue in W457hSGLT1. Thus, Trp^{457} shows the same localization as Gln^{457} which in previous studies (*4*, *34*) has been postulated to be localized in transmembrane helix XI at the interface between the membrane and the extracellular fluid.

On the other hand, the average distance from the center of the bilayer of Trp^{460} in the W460hSGLT1 mutant is only 7.4 Å (Table 6), indicating a deeper localization. Since for the lipids used in these experiments the thickness of the hydrocarbon region of the monolayer is assumed to be 15 Å, a depth of 7.4 Å from the center of the bilayer actually corresponds to the level of the tenth carbon atom of the fatty acyl chain of the phospholipid. As expected from the results reported above, we did not observe any quenching of Trp fluorescence of W602hSGLT1 or W609hSGLT1 mutants (data not shown) in these experiments, which confirms that Trp^{602} or Trp^{609} are not located within the lipid bilayer.

DISCUSSION

In the current study all experiments were performed with recombinant hSGLT1 or mutants after reconstitution. For protein reconstitution the detergent destabilization method was used (*23*, *28*, *35*). This method sometimes leads to scrambled or inside-out orientation of the transporters as reported by for example Meyer-Lipp et al. (*36*) in melibiose permease reconstitution experiments. In our case it seems that the transporters are exclusively reconstituted in a right-side-out orientation due to following reasons. First, hSGLT1 shows transport kinetics and effects of phlorizin that have been reported previously for the right-side-out orientation of hSGLT1 (*23*, *37*−*39*), as hSGLT1 in inside-out orientation shows completely different transport kinetic parameters (*40*, *41*). Second, the complete oxidation of the Trp in all mutants by *N*-bromosuccinimide−a reagent not penetrating the membrane at least under the experimental conditions employed−indicates that all Trps are facing to the extravesicular space. Third, results of trypsin bead digestion experiments on recombinant hSGLT1 reconstituted in liposomes yielded only peptides, which matched with peptides from the N-terminal domain, loop 7, and loop 9 (*42*), which in previous studies had been reported to have an extracellular orientation (*4*, *34*).

Further support for this notion that indeed transporter was reconstituted in membrane in one orientation came from NBS inability to modified Trp residues in W66hSGLT1 mutant (parallax method shows average distance of 11 Å from the center of bilayer, data not shown). This result indicates that in the current experimental setup NBS could not have modified Trp residues which are supposed to face the lumen of the proteoliposomes. However, this Trp residue is completely accessible for NBS oxidation in solution as well as in detergent treated proteoliposomes, which ruled out the possibility that this residue is buried in the protein and therefore not accessible to NBS. These data further reduce the possibility that hSGLT1 and its mutants studied in this work are reconstituted in more than one orientation, as does the fact that NBS could quench the fluorescence of all four mutants reconstituted in the proteoliposomes completely (Table 5).

As reported in previous studies, forward (*23*, *37*, *39*, *43*−*45*) and reverse transport modes (*40*, *41*, *46*) of hSGLT1 show completely different transport kinetics. In the current study we wanted to assess functional properties of the forward transport mode, i.e., outside to inside, and address ligand kinetics and critical amino acids involved in this process on the external side of the transporter; therefore we decided to perform transport kinetics and fluorescence studies of hSGLT1 and its mutants in sealed vesicles, in the absence of substrates on the trans side. In the future, reconstitution of transporter in the presence of sugars could be used to study conformations in the equilibrium exchange mode of the carrier.

In the transport studies reported above recombinant wild type hSGLT1 reconstituted into proteoliposomes shows transport characteristics very similar to the values reported in previous electrophysiological studies (*3*) performed after expression of the transporter in *Xenopus laevis* oocytes. Since it was recently demonstrated from our group (*27*) that a hSGLT1 mutant devoid of its 14 native Trps shows identical general transport properties as the wild type transporter, we thought it to be justified to use the wild type hSGLT1 for comparison with different mutants in this study.

In mutant W457hSGLT1, where Gln^{457} is replaced by Trp, the apparent affinities for different sugars decreased 10- to 30-fold, possibly due to the loss of specific interactions with Gln^{457}. This mutant also shows a marked decrease in phlorizin affinity (Table 2), which clearly indicates that D-glucose and phlorizin share common binding sites and Gln^{457} forms part of it. These conclusions are further supported by the Trp fluorescence and NBS modification studies. In fluorescence studies D-glucose and phlorizin, but not the aglucone phloretin, quenched Trp fluorescence to the same extent (Figure 4A) and both provide protection against acrylamide, KI, and TCE quenching (Table 4). NBS modification experiments (Table 5) showed similar results. The parallax method revealed an interfacial location for Trp^{457} at 10.8 Å (Table 6) from the center of the bilayer; a similar location for this residue has been postulated in previous studies (*4*, *34*).

Mutant W460hSGLT1 shows the same trend for sugar affinities as discussed above for W457hSGLT1, although the decrease in affinities is only on the order of 8- to 10-fold for sugars and 3-fold for phlorizin (Table 2). Nevertheless, the effects of sugars and phlorizin on Trp fluorescence (Table 3), the protection against quenching of Trp fluorescence by collisional quenchers in the presence of D-glucose or phlorizin (Table 4), and the shielding of Trp against NBS modification in the presence of D-glucose or phlorizin (Table 5) suggest that also Trp 460 is located in an area that forms part of the binding sites for D-glucose and the sugar moiety of phlorizin.

Mutants W602hSGLT1 and W609hSGLT1, modified in loop 13, show almost the same transport properties and the same effects of phlorizin on sugar transport as the wild type (Table 2). The positions of the Trp fluorescence emission maxima indicate a location of these residues in a very hydrophilic environment; these observations are in excellent agreements with Trp scanning studies (*21*) on isolated truncated loop 13 from rabbit SGLT1. In the presence of phlorizin both mutants exhibit a very strong quenching in Trp fluorescence with 4−5 nm red shift in the emission maxima (Figure 4C and D). Both mutants also show protection against collisional quenchers and NBS modification in the presence of phlorizin and phloretin (Table 5). Taking all these results together, it is evident that Trp^{602} and Trp^{609} provide binding sites for the aglucone part of phlorizin and phloretin.

Based on these results the question arises, why we did not observe a change in the inhibitory potency of phlorizin when the phenylalanine in these mutants was replaced with tryptophan. We, therefore, constructed two new mutants containing Ala at positions 602 and 609, and performed transport studies. These mutants exhibit almost identical transport characteristics for sugars (see Figure 2), but a very drastic decrease in the affinity for phlorizin was observed. A602hSGLT1 and A609hSGLT1 show K_i values of 58 and 45 μM *versus* 5 μM determined for hSGLT1, W602hSGLT1, or W609hSGLT1. These results underline the importance of the presence of aromatic amino acids in the phlorizin binding sites.

In the presence of D-glucose both mutants exhibited also a small protection against collisional quenchers, but no protection against NBS oxidation was observed. The small change in conformation of this area in loop 13 in the presence of D-glucose might be indirect but expected when loop 13 is indeed part of the vestibule for sugar binding of SGLT1 as postulated recently (*47*).

Molecular Basis of D-Glucose Recognition/Translocation. Importance of hydrogen bonds for sugar interaction and transport for different transporters or sugar binding proteins have been reported in the literature (*48*−*56*). Our results clearly underline the importance of residues Gln^{457} and Thr^{460} in D-glucose recognition/translocation through hSGLT1. Conservation of Gln^{457} and Thr^{460} in all known SGLT1 from different species (see Supplementary Figure 1, Supporting Information) also supports this assumption. Previous work by Diez-Sampedro et al. (*3*) assumed that hydrogen bond donation to the protein from Thr 460 to the C4 OH-group of the sugar is one of the major determining factors for sugar binding. Our transport experiments on recombinant hSGLT1 strongly support this fact as 4F4DOglc had a strikingly lower K_m compared with D-glucose (6-fold higher affinity). The orientation of the acceptor −OH group, however, does not appear to be important because the 4-epimers D-glucose and D-galactose had similar affinities. This suggests that the residue is not acidic, as commonly found in sugar-binding proteins, which do not discriminate between epimers (*51*, *52*), but contains either −OH or NH_2 group (*57*). The important role of the amino acid in this position is now demonstrated directly at the isolated carrier level as 4F4DOglc quenched Trp fluorescence to the largest extent in W460hSGLT1 with a K_d value of 0.30 mM (Table 3A). Thus it is quite probable that Thr^{460} forms a hydrogen bond with the −OH group at the C4 position of D-glucose. Similarly Gln in position 457 has been postulated from kinetics and amino acid sequence comparison to form hydrogen bonds with the C1 and C5 oxygen atom (*3*). These assumptions can now also be partly confirmed since 5-thioglucose exerts the strongest effect on the fluorescence of W457hSGLT1 with a K_d value of 39.1 mM.

In the current studies, after the introduction of Trp at positions 457 and 460, hSGLT1 is evidently still able to establish hydrogen bonds with sugars similar to the observations with Glut1 (*54*). It seems, however, that in the mutated hSGLT1, due to the bulky size of the Trp residue as compared to those of Gln or Thr, the arrangement of the hydrogen bonds is distorted. This might explain the low sugar affinities of mutant W457hSGLT1, and W460hSGLT1, but per se does not exclude the conclusions presented above, since sodium dependent D-glucose transport is observed for all mutants. Hydrodophobic interactions between sugar and different aromatic residues (Trp, Phe, and Tyr) are also widely known as important for sugar recognition and have been postulated for the sugar moiety of phlorizin in pharmacophore model studies (*58*). In lactose permease of *Escherichia coli*, Trp^{151} (*32*, *59*, *60*) plays important role in sugar recognition by hydrophobic stacking. The presence of aromatic amino acids in sugar binding sites in yeast Gal2 transporter (*61*), rat Glut1 transporter (*62*), lectins (*63*), and sugar-specific porins (*64*) has also been reported. Thus, it is quite surprising that in hSGLT1 mutation of all native Trp into Phe does not affect transport kinetics of mutant W0hSGLT1 (*27*). One possible reason for the similar transport kinetics exhibited by wild type hSGLT1 and its Trp-less mutant W0hSGLT1 might be that the replacement of amino acids is conservative in nature (Trp → Phe). The C-terminal 5-helices in hSGLT1 contain a large number of aromatic residues (5 Trp, 10 Phe, and 4 Tyr), providing potential interaction sites with the sugar; how and to what extent these amino acids influence sugar binding and specificity in hSGLT1 remains to be determined.

A Refined Model for Sugar Recognition and Phlorizin Binding. Based on our current results we can propose a refined hypothetical model for sugar recognition and phlorizin binding (see Figure 5). According to this mechanism residues Gln^{457} and Thr^{460} are present in a water-filled cavity, which can open toward the periplasm. This water filled cavity forms part of the sugar binding and translocation pathway. Presence and importance of aqueous channel in sugar permeation paths have also been reported for SGLT1 and human Glut 1 (*54*, *57*, *65*−*67*). Sodium binding to the transporter leads to conformational changes, which result in opening of this cavity to the extracellular face of the membrane (outward-facing conformation). This event has been recently demonstrated directly in single molecule recognition studies using substrate poised AFM tips (*68*). The transporter thereby interacts via Gln^{457} by hydrogen-bond bonding to O1 and O5 of the sugar; binding to Thr^{460} takes place by donation of a hydrogen bond to O4 of the sugar.

In addition, there is an interaction of the aglucone moiety of phlorizin with amino acids in the region 602 to 609. Thereby a binding pocket is created which as predicted from the studies by Wielert-Badt et al. (*58*) is larger than the glucose binding pocket. Wielert-Badt et al. (*58*) also

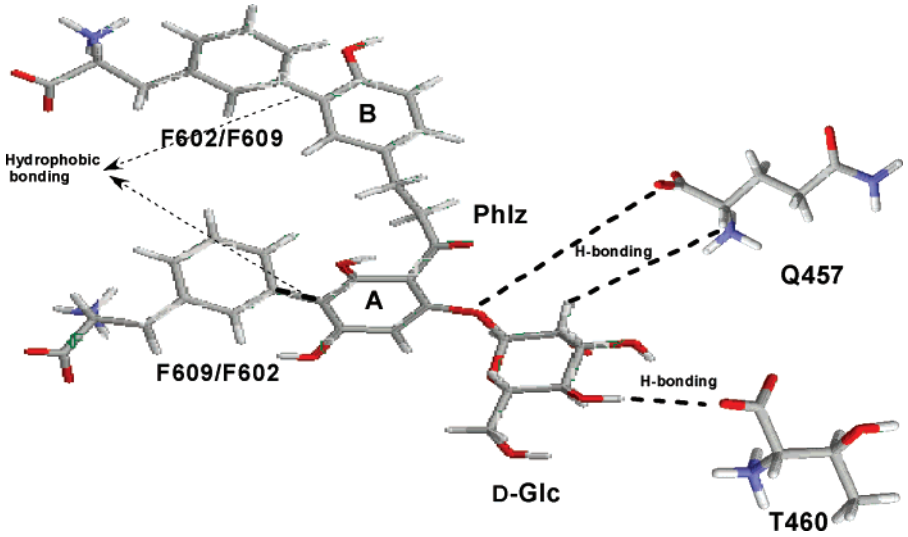

FIGURE 5: Hypothetical scheme of major interaction sites between phlorizin and hSGLT1. The sugar moiety of phlorizin interacts with residues $Gln^{457}$and Thr^{460} present in TMH XI probably by the same hydrogen bond interactions as D-glucose does; the aromatic ring A of the aglucone interacts with Phe^{609}/Phe^{602}, and ring B makes contact with Phe^{602}/Phe^{609}; both are present in the extracellular loop 13 of hSGLT1. (For details see Discussion.)

concluded that in addition to hydrophobic interactions hydrogen bond formation at the 4 and 6-OH groups of the aromatic ring A are essential for phlorizin binding. The red shift in the fluorescence emission maximum of W602hSGLT1 and W609hSGLT1 in the presence of phlorizin indicates a transition from an ordered state to a less ordered state of loop 13 of hSGLT1. A similar finding for different Trp mutants of truncated loop 13 has been reported in previous studies from our group (*21*). However, the shift in the maximum of Trp fluorescence toward a longer wavelength could also be caused by a strong interaction of phlorizin-associated water with loop 13 of hSGLT1. Such a complex between phlorizin and water molecules can be formed by H-bonding between −OH groups of phlorizin aromatic ring A. The aromatic ring B of phlorizin interacts probably with residue Phe^{602}/Phe^{609}. The results of our photolabeling experiments on truncated loop 13 of rabbit SGLT1 with 3-azido phlorizin with the reactive azido group on ring B suggest an interaction at this position (*21*). In intact rabbit SGLT1 a similar location for phlorizin binding sites has been reported (*18*, *20*). However, a recent study from Gagnon et al. (*19*) on hSGLT1 claimed that the phlorizin binding site is not located between residues 602 and 611. The discrepancy between our current study and the results of Gagnon et al. (*19*) might be that in their studies residues Phe^{602} and Phe^{609} were not investigated directly and separately.

Thus, in summary, the binding site for the aglucone moiety for phlorizin is located between residues 602 and 609, where Phe^{602} and Phe^{609} form part of the binding site; in this region ring A interacts with Phe^{609}/Phe^{602} via hydrogen bonds; ring B does so with Phe^{602}/ Phe^{609} via hydrophobic interactions. The sugar moiety of phlorizin is free to interact with Gln^{457} and Thr^{460} residues present in the D-glucose binding site (Figure 5). The proposed mechanism can easily explain competitive inhibition of sugar transport by phlorizin and its 500-fold higher affinity toward hSGLT1 (*14*, *17*) compared to D-glucose.

The studies on the location of the Trp within the membrane by the parallax method lead to further conclusions. The water filled cavity extends by 5−7 Å into the membrane, and is part of the phlorizin binding site whose dimensions have been estimated to be 10 × 17 × 7 Å. This requires that the domains of loop 13 between 602 and 609 have to come into very close vicinity to the membrane when the carrier−phlorizin complex is formed. Such a "contraction'' of the transporter has been implied already in the single molecule recognition experiments by Wielert-Badt et al. (*69*) and by the studies on the conformation of recombinant hSGLT1 in solution and after reconstitution into proteoliposomes (*23*, *24*). Clearly these considerations have to be verified—or falsified—by crystallization studies which unfortunately have been possible thus far only for a limited number of membrane transporters (*49*, *50*).

SUPPORTING INFORMATION AVAILABLE

Supplementary Figure 1 showing the amino acid sequence alignment of SGLT1 from different species. Sequences are identified with the NCBI accession numbers, and sequence alignments are performed by using the ClustalW program (http://www.ebi.ac.uk/clustalw). This material is available free of charge via the Internet at http://pubs.acs.org.

REFERENCES

1. Wood, I. S., and Trayhurn, P. (2003) Glucose transporters (GLUT and SGLT): expanded families of sugar transport proteins, *Br. J. Nutr. 89*, 3−9.
2. Wright, E. M., Loo, D. D., Turk, E., and Hirayama, B. A. (1996) Sodium cotransporters, *Curr. Opin. Cell Biol. 8*, 468−473.
3. Diez-Sampedro, A., Wright, E. M., and Hirayama, B. A. (2001) Residue 457 controls sugar binding and transport in the Na^+/glucose cotransporter, *J. Biol. Chem. 276*, 49188−49194.
4. Turk, E., and Wright, E. M. (1997) Membrane topology motifs in the SGLT cotransporter family, *J. Membr. Biol. 159*, 1−20.
5. Meinild, A. K., Loo, D. D., Hirayama, B. A., Gallardo, E., and Wright, E. M. (2001) Evidence for the involvement of Ala 166 in coupling Na^+ to sugar transport through the human Na^+/glucose cotransporter, *Biochemistry 40*, 11897−11904.
6. Panayotova-Heiermann, M., Loo, D. D., Kong, C. T., Lever, J. E., and Wright, E. M. (1996) Sugar binding to Na^+/glucose cotransporters is determined by the carboxyl-terminal half of the protein, *J. Biol. Chem. 271*, 10029−10034.
7. Panayotova-Heiermann, M., Eskandari, S., Turk, E., Zampighi, G. A., and Wright, E. M. (1997) Five transmembrane helices form

the sugar pathway through the Na^+/glucose cotransporter, *J. Biol. Chem. 272*, 20324−20327.
8. Diez-Sampedro, A., Loo, D. D., Wright, E. M., Zampighi, G. A., and Hirayama, B. A. (2004) Coupled sodium/glucose cotransport by SGLT1 requires a negative charge at position 454, *Biochemistry 43*, 13175−13184.
9. Martin, M. G., Turk, E., Lostao, M. P., Kerner, C., and Wright, E. M. (1996) Defects in Na^+/glucose cotransporter (SGLT1) trafficking and function cause glucose-galactose malabsorption, *Nat. Genet. 12*, 216−220.
10. Mirza, O., Guan, L., Verner, G., Iwata, S., and Kaback, H. R. (2006) Structural evidence for induced fit and a mechanism for sugar/H^+ symport in LacY, *EMBO J. 25*, 1177−1183.
11. Stockner, T., Vogel, H. J., and Tieleman, D. P. (2005) A salt-bridge motif involved in ligand binding and large-scale domain motions of the maltose-binding protein, *Biophys. J. 89*, 3362−3371.
12. Dumas, F., Koebnik, R., Winterhalter, M., and Van Gelder, P. (2000) Sugar transport through maltoporin of *Escherichia coli*. Role of polar tracks, *J. Biol. Chem. 275*, 19747−19751.
13. Panayotova-Heiermann, M., Loo, D. D., Lam, J. T., and Wright, E. M. (1998) Neutralization of conservative charged transmembrane residues in the Na^+/glucose cotransporter SGLT1, *Biochemistry 37*, 10522−10528.
14. Diedrich, D. F. (1966) Competitive inhibition of intestinal glucose transport by phlorizin analogs, *Arch. Biochem. Biophys. 117*, 248−256.
15. Oulianova, N., Falk, S., and Berteloot, A. (2001) Two-step mechanism of phlorizin binding to the SGLT1 protein in the kidney, *J. Membr. Biol. 179*, 223−242.
16. Oulianova, N., and Berteloot, A. (1996) Sugar transport heterogeneity in the kidney: two independent transporters or different transport modes through an oligomeric protein? 1. Glucose transport studies, *J. Membr. Biol. 153*, 181−194.
17. Hirayama, B. A., Diez-Sampedro, A., and Wright, E. M. (2001) Common mechanisms of inhibition for the Na^+/glucose (hSGLT1) and Na^+/Cl^-/GABA (hGAT1) cotransporters, *Br. J. Pharmacol. 134*, 484−495.
18. Novakova, R., Homerova, D., Kinne, R. K., Kinne-Saffran, E., and Lin, J. T. (2001) Identification of a region critically involved in the interaction of phlorizin with the rabbit sodium-D-glucose cotransporter SGLT1, *J. Membr. Biol. 184*, 55−60.
19. Gagnon, D. G., Holt, A., Bourgeois, F., Wallendorff, B., Coady, M. J., and Lapointe, J. Y. (2005) Membrane topology of loop 13−14 of the Na^+/glucose cotransporter (SGLT1): A SCAM and fluorescent labeling study, *Biochim. Biophys. Acta 1712*, 173−184.
20. Xia, X., Lin, J. T., and Kinne, R. K. (2003) Binding of phlorizin to the isolated C-terminal extramembranous loop of the Na^+/glucose cotransporter assessed by intrinsic tryptophan fluorescence, *Biochemistry 42*, 6115−6120.
21. Raja, M. M., Tyagi, N. K., and Kinne, R. K. (2003) Phlorizin recognition in a C-terminal fragment of SGLT1 studied by tryptophan scanning and affinity labeling, *J. Biol. Chem. 278*, 49154−49163.
22. Raja, M. M., Kipp, H., and Kinne, R. K. (2004) C-terminus loop 13 of Na^+ glucose cotransporter SGLT1 contains a binding site for alkyl glucosides, *Biochemistry 43*, 10944−10951.
23. Tyagi, N. K., Goyal, P., Kumar, A., Pandey, D., Siess, W., and Kinne, R. K. (2005) High-yield functional expression of human sodium/D-glucose cotransporter1 in *Pichia pastoris* and characterization of ligand-induced conformational changes as studied by tryptophan fluorescence, *Biochemistry 44*, 15514−15524.
24. Kumar, A., Tyagi, N. K., and Kinne, R. K. (2007) Ligand-mediated conformational changes and positioning of tryptophans in reconstituted human sodium/D-glucose cotransporter1 (hSGLT1) probed by tryptophan fluorescence, *Biophys. Chem. 127*, 69−77.
25. Loo, D. D., Hirayama, B. A., Gallardo, E. M., Lam, J. T., Turk, E., and Wright, E. M. (1998) Conformational changes couple Na^+ and glucose transport, *Proc. Natl. Acad. Sci. U.S.A. 95*, 7789−7794.
26. Meinild, A. K., Hirayama, B. A., Wright, E. M., and Loo, D. D. (2002) Fluorescence studies of ligand-induced conformational changes of the Na^+/glucose cotransporter, *Biochemistry 41*, 1250−1258.
27. Kumar, A., Tyagi, N. K., Goyal, P., Pandey, D., Siess, W., and Kinne, R. K. (2007) Sodium-independent low-affinity D-glucose transport by human sodium/ D -glucose cotransporter 1: Critical role of tryptophan 561, *Biochemistry 46*, 2758−2766.
28. Rigaud, J. L., and Levy, D. (2003) Reconstitution of membrane proteins into liposomes, *Methods Enzymol. 372*, 65−86.
29. Holloway, P. W. (1973) A simple procedure for removal of Triton X-100 from protein samples, *Anal. Biochem. 53*, 304−308.
30. Chattopadhyay, A., and London, E. (1987) Parallax method for direct measurement of membrane penetration depth utilizing fluorescence quenching by spin-labeled phospholipids, *Biochemistry 26*, 39−45.
31. Abrams, F. S., Chattopadhyay, A., and London, E. (1992) Determination of the location of fluorescent probes attached to fatty acids using parallax analysis of fluorescence quenching: Effect of carboxyl ionization state and environment on depth, *Biochemistry 31*, 5322−5327.
32. Vazquez-Ibar, J. L., Guan, L., Svrakic, M., and Kaback, H. R. (2003) Exploiting luminescence spectroscopy to elucidate the interaction between sugar and a tryptophan residue in the lactose permease of *Escherichia coli*, *Proc. Natl. Acad. Sci. U.S.A. 100*, 12706−12711.
33. Carr, A. C., Winterbourn, C. C., and van den Berg, J. J. (1996) Peroxidase-mediated bromination of unsaturated fatty acids to form bromohydrins, *Arch. Biochem. Biophys. 327*, 227−233.
34. Turk, E., Kerner, C. J., Lostao, M. P., and Wright, E. M. (1996) Membrane topology of the human Na^+/glucose cotransporter SGLT1, *J. Biol. Chem. 271*, 1925−1934.
35. Rigaud, J. L., Pitard, B., and Levy, D. (1995) Reconstitution of membrane proteins into liposomes: application to energy-transducing membrane proteins, *Biochim. Biophys. Acta 1231*, 223−246.
36. Meyer-Lipp, K., Sery, N., Ganea, C., Basquin, C., Fendler, K., and Leblanc, G. (2006) The inner interhelix loop 4−5 of the melibiose permease from *Escherichia coli* takes part in conformational changes after sugar binding, *J. Biol. Chem. 281*, 25882−25892.
37. Quick, M., and Wright, E. M. (2002) Employing *Escherichia coli* to functionally express, purify, and characterize a human transporter, *Proc. Natl. Acad. Sci. U.S.A. 99*, 8597−8601.
38. Kinne, R. (1976) Properties of the glucose transport system in the renal brush border membrane, *Curr. Top. Membr. Transp. 8*, 209−267.
39. Lin, J. T., Kormanec, J., Wehner, F., Wielert-Badt, S., and Kinne, R. K. (1998) High-level expression of Na^+/D-glucose cotransporter (SGLT1) in a stably transfected Chinese hamster ovary cell line, *Biochim. Biophys. Acta 1373*, 309−320.
40. Firnges, M. A., Lin, J. T., and Kinne, R. K. (2001) Functional asymmetry of the sodium-D-glucose cotransporter expressed in yeast secretory vesicles, *J. Membr. Biol. 179*, 143−153.
41. Quick, M., Tomasevic, J., and Wright, E. M. (2003) Functional asymmetry of the human Na^+/glucose transporter (hSGLT1) in bacterial membrane vesicles, *Biochemistry 42*, 9147−9152.
42. Kumar, A., Tyagi, N. K., Arevalo, E., Miller, K. W., and Kinne, R. K. (2007) A proteomic study of sodium/D-glucose cotransporter 1 (SGLT1): Topology of loop 13 and coverage of other functionally important domains, *Biochim. Biophys. Acta 1774*, 968−974.
43. Schultz, S. G., and Curran, P. F. (1970) Coupled transport of sodium and organic solutes, Characterization of a Na^+/glucose cotransporter cloned from rabbit small intestine, *Physiol Rev 50*, 637−718.
44. Ikeda, T. S., Hwang, E. S., Coady, M. J., Hirayama, B. A., Hediger, M. A., and Wright, E. M. (1989) Characterization of a Na^+/glucose cotransporter cloned from rabbit small intestine, *J. Membr. Biol. 110*, 87−95.
45. Hediger, M. A., Coady, M. J., Ikeda, T. S., and Wright, E. M. (1987) Expression cloning and cDNA sequencing of the Na^+/glucose co-transporter, *Nature 330*, 379−381.
46. Sauer, G. A., Nagel, G., Koepsell, H., Bamberg, E., and Hartung, K. (2000) Voltage and substrate dependence of the inverse transport mode of the rabbit Na^+/glucose cotransporter (SGLT1), *FEBS Lett. 469*, 98−100.
47. Puntheeranurak, T., Kasch, M., Xia, X., Hinterdorfer, P., and Kinne, R. K. (2007) Three surface subdomains form the vestibule of the Na^+/glucose cotransporter SGLT1, *J. Biol. Chem. 282*, 25222−25230.
48. Jeffrey, G. A. (1997) *An introduction to hydrogen bonding*, Oxford University Press, New York 1977.
49. Abramson, J., Smirnova, I., Kasho, V., Verner, G., Kaback, H. R., and Iwata, S. (2003) Structure and mechanism of the lactose permease of *Escherichia coli*, *Science 301*, 610−615.

50. Huang, Y., Lemieux, M. J., Song, J., Auer, M., and Wang, D. N. (2003) Structure and mechanism of the glycerol-3-phosphate transporter from *Escherichia coli*, *Science 301*, 616−620.
51. Quiocho, F. A., Vyas, N. K., Sack, J. S., and Vyas, M. N. (1987) Atomic protein structures reveal basic features of binding of sugars and ionic substrates, and calcium cation, *Cold Spring Harbor Symp. Quant. Biol. 52*, 453−463.
52. Quiocho, F. A., and Vyas, N. K. (1984) Novel stereospecificity of the L-arabinose-binding protein, *Nature 310*, 381−386.
53. Quiocho, F. A., Wilson, D. K., and Vyas, N. K. (1989) Substrate specificity and affinity of a protein modulated by bound water molecules, *Nature 340*, 404−407.
54. Salas-Burgos, A., Iserovich, P., Zuniga, F., Vera, J. C., and Fischbarg, J. (2004) Predicting the three-dimensional structure of the human facilitative glucose transporter glut1 by a novel evolutionary homology strategy: insights on the molecular mechanism of substrate migration, and binding sites for glucose and inhibitory molecules, *Biophys. J. 87*, 2990−2999.
55. Bejar, C. M., Jin, X., Ballicora, M. A., and Preiss, J. (2006) Molecular architecture of the glucose 1-phosphate site in ADP-glucose pyrophosphorylases, *J. Biol. Chem. 281*, 40473−40484.
56. Kasahara, T., Ishiguro, M., and Kasahara, M. (2006) Eight amino acid residues in transmembrane segments of yeast glucose transporter Hxt2 are required for high affinity transport, *J. Biol. Chem. 281*, 18532−18538.
57. Hashiramoto, M., Kadowaki, T., Clark, A. E., Muraoka, A., Momomura, K., Sakura, H., Tobe, K., Akanuma, Y., Yazaki, Y., Holman, G. D., and et al. (1992) Site-directed mutagenesis of GLUT1 in helix 7 residue 282 results in perturbation of exofacial ligand binding, *J. Biol. Chem. 267*, 17502−17507.
58. Wielert-Badt, S., Lin, J. T., Lorenz, M., Fritz, S., and Kinne, R. K. (2000) Probing the conformation of the sugar transport inhibitor phlorizin by 2D-NMR, molecular dynamics studies, and pharmacophore analysis, *J. Med. Chem. 43*, 1692−1698.
59. Vazquez-Ibar, J. L., Guan, L., Weinglass, A. B., Verner, G., Gordillo, R., and Kaback, H. R. (2004) Sugar recognition by the lactose permease of *Escherichia coli*, *J. Biol. Chem. 279*, 49214−49221.
60. Guan, L., Hu, Y., and Kaback, H. R. (2003) Aromatic stacking in the sugar binding site of the lactose permease, *Biochemistry 42*, 1377−1382.
61. Kasahara, T., and Kasahara, M. (2000) Three aromatic amino acid residues critical for galactose transport in yeast Gal2 transporter, *J. Biol. Chem. 275*, 4422−4428.
62. Kasahara, T., and Kasahara, M. (1998) Tryptophan 388 in putative transmembrane segment 10 of the rat glucose transporter Glut1 is essential for glucose transport, *J. Biol. Chem. 273*, 29113−29117.
63. Weis, W. I., and Drickamer, K. (1996) Structural basis of lectin-carbohydrate recognition, *Annu. Rev. Biochem. 65*, 441−473.
64. Forst, D., Welte, W., Wacker, T., and Diederichs, K. (1998) Structure of the sucrose-specific porin ScrY from *Salmonella typhimurium* and its complex with sucrose, *Nat. Struct. Biol. 5*, 37−46.
65. Wright, E. M., and Turk, E. (2004) The sodium/glucose cotransport family SLC5, *Pfluegers Arch. 447*, 510−518.
66. Mori, H., Hashiramoto, M., Clark, A. E., Yang, J., Muraoka, A., Tamori, Y., Kasuga, M., and Holman, G. D. (1994) Substitution of tyrosine 293 of GLUT1 locks the transporter into an outward facing conformation, *J. Biol. Chem. 269*, 11578−11583.
67. Hruz, P. W., and Mueckler, M. M. (1999) Cysteine-scanning mutagenesis of transmembrane segment 7 of the GLUT1 glucose transporter, *J. Biol. Chem. 274*, 36176−36180.
68. Puntheeranurak, T., Wildling, L., Gruber, H. J., Kinne, R. K., and Hinterdorfer, P. (2006) Ligands on the string: single-molecule AFM studies on the interaction of antibodies and substrates with the Na^+-glucose co-transporter SGLT1 in living cells, *J. Cell Sci. 119*, 2960−2967.
69. Wielert-Badt, S., Hinterdorfer, P., Gruber, H. J., Lin, J. T., Badt, D., Wimmer, B., Schindler, H., and Kinne, R. K. (2002) Single molecule recognition of protein binding epitopes in brush border membranes by force microscopy, *Biophys. J. 82*, 2767−2774.

BI701193X